Indian Journal of Marine Sciences
Vol. 27, March 1998, pp. 104-114

Various approaches to the modelling of large scale 3-dimensional circulation in the ocean

C Shaji, N Bahulayan*, A D Rao & S K Dube
Centre for Atmospheric Sciences, Indian Institute of Technology, New Delhi 110016, India
*Physical Oceanography Division, National Institute of Oceanography, Goa 403004, India

Received 23 May 1997; revised 10 December 1997

In this paper, the three different approaches to the modelling of large scale 3-dimensional flow in the ocean such as the diagnostic, semi-diagnostic (adaptation) and the prognostic are discussed in detail. Three-dimensional solutions are obtained for the circulation during winter of the western part of Indian Ocean north of 20°S and west of 80°E using diagnostic and semi-diagnostic models. Both the models computed realistically well the persistent major currents during winter in the upper levels of the ocean. The semi-diagnostic calculations showed that the velocity fields were smoothed and unrealistic currents were removed in the model domain, especially in the Somali and equatorial regions during the adaptation stage. Temperature and salinity anomaly fields showed that the climatic temperature and salinity data used to drive the model has also been smoothed considerably during the adaptation stage.

The initial data play a crucial role in forecasting ocean currents. The number of hydrological stations is so small that direct measurements cannot provide a complete description of the large scale circulation. However, dynamical synthesis and interpretation of data can be achieved by a variety of diagnostic, semi-diagnostic and prognostic models. The main objectives of a mathematical modeler are to identify the forcing functions that control the large scale variability of circulation, to simulate the mean circulation and to predict the circulation on time scales of months to seasons. Prediction of circulation is required for the prediction of climate on time scales of seasons to years.

The three broad categories of large scale 3-dimensional ocean circulation modelling approach such as the diagnostic, semi-diagnostic and prognostic are discussed in detail in this paper. Also present are some computational results of the 3-dimensional flow in the western part of the tropical Indian Ocean using diagnostic and semi-diagnostic models.

Materials and Methods

Modelling of large scale 3-dimensional flow in the ocean can be broadly classified as (a) diagnostic modelling (b) semi-diagnostic or adaptation modelling (c) prognostic modelling.

Diagnostic modelling

In a diagnostic model, all the equations of prognostic model except the equations of temperature and salinity are used to study the steady state circulation of a particular area. The internal density field, which is part of the model equations, is imposed on the model from observations of temperature and salinity and is not predicted as part of the model calculation. This method was extensively applied in the North Atlantic region where observed density data were available at specific space intervals. The main advantage of the diagnostic model is that it takes only a small fraction of the computer time of the prognostic model. The model ocean reaches a state of statistical equilibrium in about one to two months instead of several hundred years of model time of prognostic models. Diagnostic calculation results are used to construct atlases of horizontal and vertical circulations in the seas and oceans. The diagnostic calculations are not good if the density field is greatly smoothed or the density field contain significant errors. Further, in the diagnostic method the imposed density field is not in adjustment with wind stress, flow field and bottom topography. Many diagnostic calculations of seasonal mean currents in the non-equatorial regions of the world

oceans have been carried out by Sarkisyan and his co-workers[1-5].

Semi-diagnostic or adaptation modelling

One of the main drawbacks of the diagnostic model is that the observed density field used to drive the model is not hydrodynamically adjusted with the flow field, wind stress and bottom topography. In order to overcome the drawbacks of diagnostic models, Sarkisyan & Demin[6], for the first time, developed a new technique called semi-diagnostic technique to calculate the steady state 3-dimensional circulation. In semi-diagnostic models, the adjustment of observed data with model equations, boundary conditions and basin geometry takes place.

The numerical solution of semi-diagnostic models are completed in two stages: the first stage is called the diagnostic stage and the second stage is called initialisation or adaptation or adjustment. In the diagnostic stage only the diagnostic model equations of momentum, hydrostatics, continuity and the equation for the integral function are solved subject to proper boundary and initial conditions. The initial state for the velocity field is a state of rest. The diagnostic computations are continued only till the flow field is generated and it is not essential to continue the computations till full steady state is reached. In the second stage, after having generated the flow fields diagnostically, the equations of diagnostic model together with the equations of heat and salt are again solved, using the flow field obtained from diagnostic stage and original temperature and salinity fields (based on observations) as initial conditions. The integration of model equations are again continued for approximately another one month during which the observed density field is allowed to vary to a certain extent and the flow fields are hydrodynamically adjusted with the wind stress and bottom topography. Marchuk & Sarkisyan[7] published a brief analysis of the results of semi-diagnostic calculation of currents in the North Atlantic and Black Sea areas.

Prognostic modelling

In prognostic modelling, classical ocean hydrothermodynamic equations that govern the large scale motions in the sea are written in a form suitable for numerical solution using a digital computer. The model is driven by classical boundary conditions which are time-dependent. Observations are employed only to provide boundary and initial conditions and also for the validation of model results. All the internal fields in the ocean such as velocity components, density field, temperature and salinity fields are evolved with respect to time and space from solutions of model equations. One disadvantage of the prognostic model is that it takes considerable computer time to obtain a statistically stable equilibrium solution. Normally, the integration of model equations should be continued for many years and sometimes even centuries of model time. One of the main advantages of prognostic model is that only limited data for prescribing boundary and initial conditions are required to formulate and develop the model.

Results and Discussion

Results of diagnostic calculations of currents in the western tropical Indian Ocean

The basic hydrodynamic equations in spherical co-ordinate system governing the large scale 3-dimensional flow in the ocean were taken from Gill[8]. These equations are then modified in terms of the co-latitude of the place and particular sign convention used wherein the longitude (λ) increases towards east, the co-latitude (θ) increases towards south and the vertical co-ordinate (z) increases downwards. The model consists of 33 levels in the vertical which are standard oceanographic depths and a resolution of 1° in the zonal and meridional directions. The final model equations for the hydrodynamics of the ocean in the approximations of Boussinesq, hydrostatics and incompressibility of seawater are of the following form:

Equations of motion:

$$\frac{\partial u}{\partial t} + Au + lv + \cot\theta \frac{uv}{R} = -\frac{1}{\rho_o R \sin\theta} \frac{\partial p}{\partial \lambda} + F^{\lambda} \quad \ldots (1)$$

$$\frac{\partial v}{\partial t} + Av - lu - \cot\theta \frac{u^2}{R} = -\frac{1}{\rho_o R} \frac{\partial p}{\partial \theta} + F^{\theta} \quad \ldots (2)$$

Hydrostatic equation:

$$\frac{\partial p}{\partial z} = g\rho \qquad \ldots (3)$$

Equation of continuity:

$$\frac{1}{R\sin\theta}\left[\frac{\partial u}{\partial \lambda}+\frac{\partial(v\sin\theta)}{\partial\theta}\right]+\frac{\partial w}{\partial z} = 0 \qquad \ldots (4)$$

Density of seawater is calculated from observations of temperature and salinity using the following equation of state:

$$\rho = \rho(T,S) \qquad \ldots (5)$$

The density of seawater, ρ, is usually written in terms of another variable called sigma-t (σ_t) in the following form:

$$\sigma_t = (\rho-1)1000 \qquad \ldots (5)$$

where

θ	—co-latitude = 90-ϕ, ϕ is the latitude.
u,v,w	—the velocity components along the east(λ), south(θ) and downward(z) directions respectively.
p	—hydrostatic pressure.
ρ	—density of seawater.
ρ_0	—constant density.
R	—radius of the Earth.
l	—$2\Omega\cos\theta$.
Ω	—angular velocity of Earth's rotation.
Au, Av	—advective acceleration terms.
F^λ, F^θ	—friction terms in the momentum equations.
μ, ν	—horizontal and vertical turbulent mixing coefficients respectively.
T	—temperature.
S	—salinity.

$$Af = (Au, Av) = \frac{1}{R\sin\theta}\left[\frac{\partial(uf)}{\partial\lambda}+v\frac{\partial(f\sin\theta)}{\partial\theta}\right] + \frac{\partial(wf)}{\partial z}$$

$$F^\lambda = \frac{\partial\left(\nu\frac{\partial u}{\partial z}\right)}{\partial z}+\mu\left[\Delta u-\frac{u}{R^2\sin^2\theta}+\frac{2\cos\theta}{R^2\sin^2\theta}\frac{\partial v}{\partial\lambda}\right]$$

$$F^\theta = \frac{\partial\left(\nu\frac{\partial v}{\partial z}\right)}{\partial z}+\mu\left[\Delta v-\frac{v}{R^2\sin^2\theta}+\frac{2\cos\theta}{R^2\sin^2\theta}\frac{\partial u}{\partial\lambda}\right]$$

$$\Delta f = (\Delta u, \Delta v) = \frac{1}{R^2\sin^2\theta}\frac{\partial^2 f}{\partial\lambda^2} + \frac{1}{R^2\sin\theta}\frac{\partial\left(\sin\theta\frac{\partial f}{\partial\theta}\right)}{\partial\theta}$$

The boundary and initial conditions used for the solution of the model equations are of the following form:

At the sea surface (z=0), the following boundary conditions were employed for the velocity fields.

$$\rho_0\nu\frac{\partial u}{\partial z} = -\tau_\lambda;\ \rho_0\nu\frac{\partial v}{\partial z} = -\tau_\theta;\ w|_{z=0} = 0 \qquad \ldots (6)$$

where τ_λ and τ_θ are the components of wind stress in the zonal and meridional directions respectively and u,v are the components of velocity fields.

At the sea bottom z=H(λ,θ), no-slip boundary condition for velocity fields was applied .

i. e. $u = v = w = 0$ ... (7)

Along the rigid lateral (coastal) boundaries of the model, the normal flux boundary conditions of zero velocity is prescribed.

i.e. $\vec{V}_n = 0$ ... (8)

where 'n' is the normal to the lateral boundary.

A quasi-geostrophic model of Marchuk & Sarkisyan[7] was used to compute the velocity components at all the levels along the open boundaries of the model. The prescribed velocity components were kept constant throughout the model integration.

An initial state of rest is prescribed for the velocity components u and v before starting the integration.

i.e. $(u,v)_{t=0} = 0$ ... (9)

The density of sea water 'ρ' is assumed to be the sum of a constant density 'ρ_0' and the density anomaly (ρ(λ,θ,z). Integrating the hydrostatic Eq. (3) in the vertical from free surface to depth, the expression for hydrostatic pressure at depth z can be written as:

$$p_z = \rho_0 g\zeta + g\int_0^z \rho' dz \qquad \ldots (10)$$

where 'ζ' is the sea surface topography which is

otherwise called sea level. The unknowns in the model equations are the velocity components (u,v,w), pressure (p) and sea level (ζ). The Eqs (1-4) taking into account the equation for hydrostatic pressure Eq. (10) were solved with the help of a leap-frog numerical scheme.

The sea level equation is obtained from the finite-difference equations of momentum, hydrostatics and continuity. The two-dimensional integral continuity equation, which is the equation for sea surface topography at the internal grid points, is obtained by summing up the equation of continuity along all vertical levels, taking into consideration the boundary condition for vertical velocity ($w = 0$) at the surface and bottom. By applying the lateral boundary condition for velocity fields, the equation for sea surface topography at the solid boundary points are also obtained. The sea level equation is solved by successive overrelaxation technique. A detailed discussion on the derivation of sea surface topography equation is given in the works of Bahulayan & Shaji[9].

Numerical solution procedure

The hydrodynamic Eqs (1-4) and the sea surface topography equation were solved on a 46×51 staggered grid with the appropriate boundary and initial conditions mentioned above. The equation of state (Eq. 5) is used to compute the density field and the same is kept constant throughout the model integration. Equations are integrated forward in time with a time step of 1 hour for approximately one month by which time the flow fields are generated completely. The horizontal and vertical eddy viscosity coefficients used in the model are 5×10^8 cm^2 sec^{-1} and 10 cm^2 sec^{-1} respectively. Model computed sea level and the circulation at 20, 50, 150, 300, 500 and 1000 m depths in the upper levels of the ocean during winter season is discussed in the following sections.

Model input

The wind stress and density fields (σ_t) are provided from the climatology of Hellerman & Rosenstein[10] and Levitus[11] respectively to drive the model. Figure 1 represents the resultant wind field during winter. The strength of northeasterly winds are very high off the Somali region. Very weak westerly and northwesterly winds are observed north of 20°N latitude. SE trades prevail in the Southern Hemisphere between 10 and 20°S latitude. There is very weak northerly, westerly and northwesterly winds between equator and 10°S, east of 55°E.

Figure 2 depicts the F_t fields at 20, 50, 150, 300, 500 and 1000 m depths during winter season. At 20 m depth, high dense water is found in the Arabian Sea north of 15°N (Fig. 2a) with σ_t value reaching up to 24.2. The density decreases gradually towards the equatorial region and low dense water with σ_t of 22.0 is observed in the equatorial Indian Ocean. Density is further reduced off the south west coast of India due to the presence of less saline Bay of Bengal water advected to this region. At 50 m depth (Fig. 2b), the density again decreases from north to south with high dense water in the northern Arabian Sea and low dense water in the equatorial region. In general, low dense water is observed south of the equator compared to the Northern Hemisphere. At 150 m depth, σ_t decreases from north to south in the northern Arabian Sea (Fig. 2c), however the density

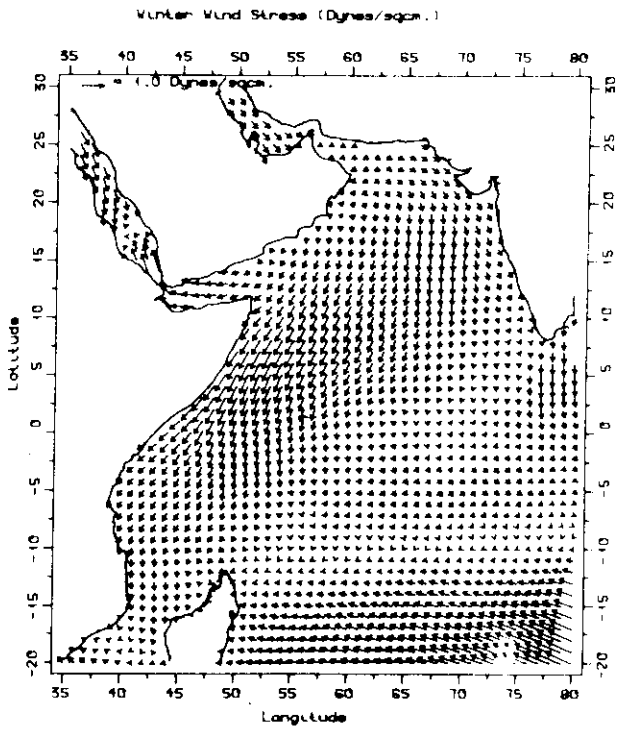

Fig. 1—Distribution of resultant wind stress (dynes cm^{-2}) during winter season.

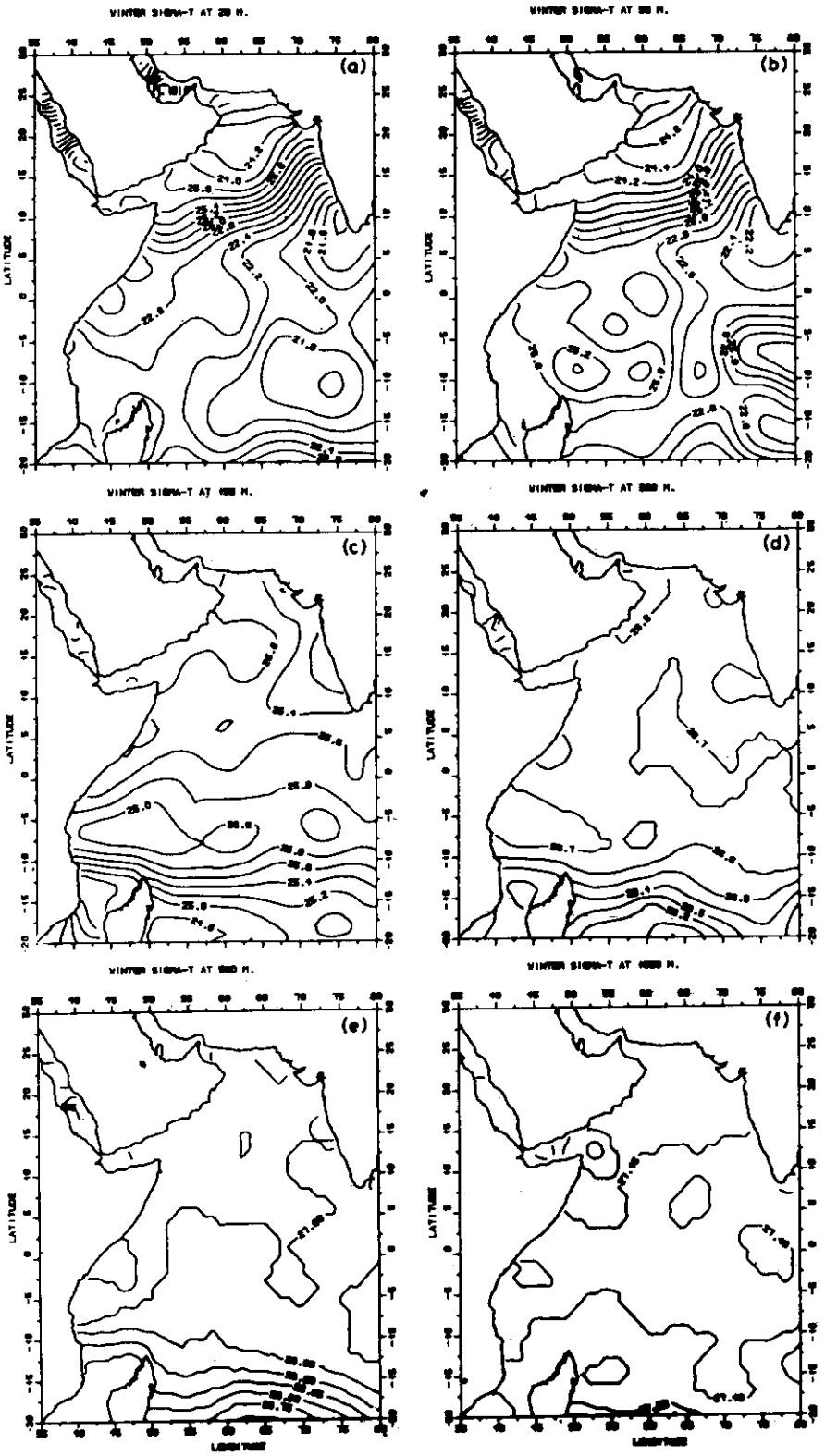

Fig. 2—The σ_t fields during winter season at (a) 20 m depth (b) 50 m depth (c) 150 m (d) 300 m (e) 500 m (f) 1000 m depths.

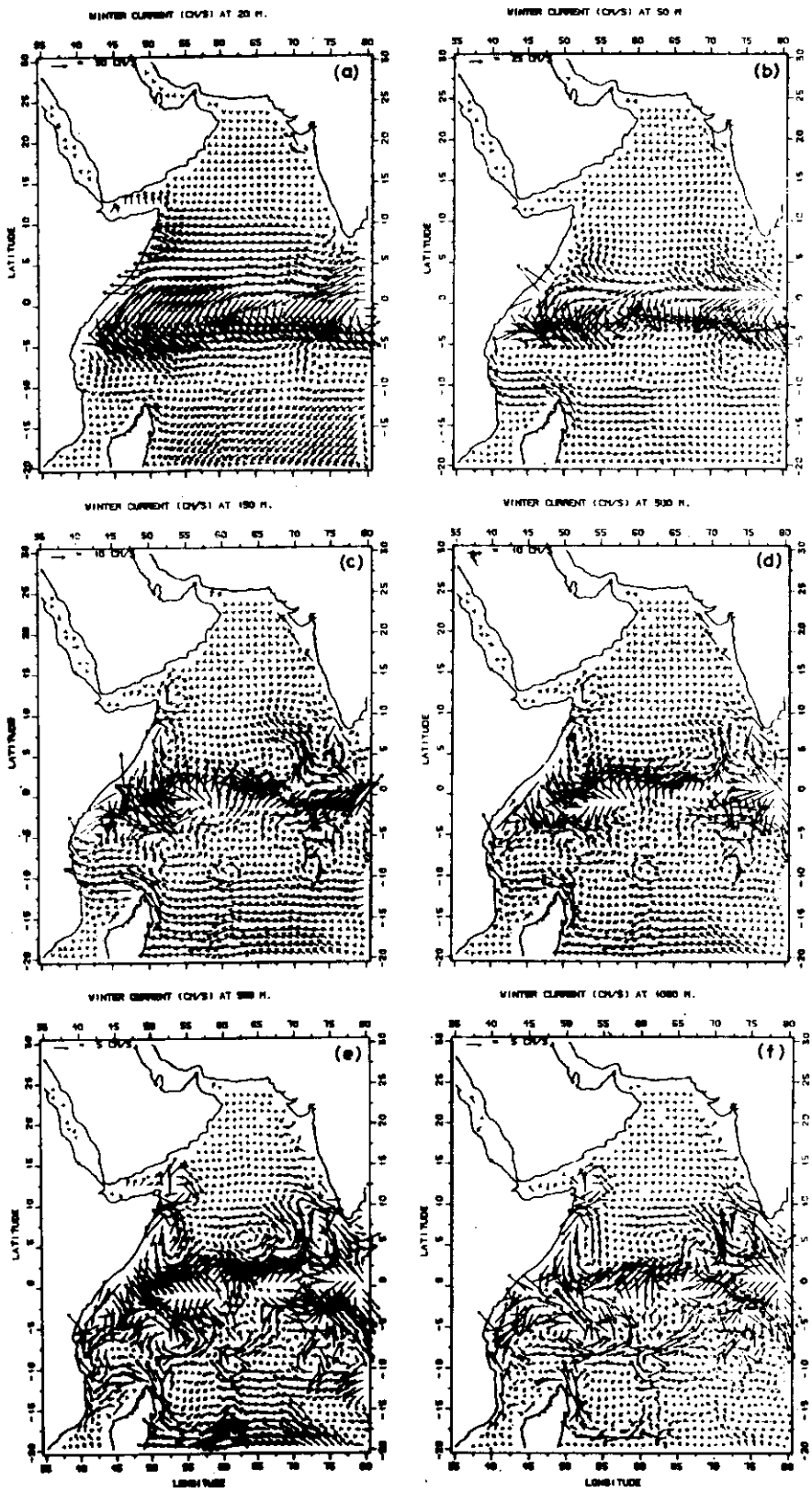

Fig. 3—Computed currents (cm sec^{-1}) during winter season using diagnostic model at (a) 20 m depth (b) 50 m depth (c) 150 m (d) 300 m (e) 500 m (f) 1000 m depths.

gradient is very less. High dense water is found in the equatorial region at this depth. There is no appreciable change in the σ_t values at 300 m in the entire model domain (Fig. 2d), except a gradual density gradient south of 10°S latitude. At 150 and 300 m depths, south of 10°S, the F_t lines are more or less oriented in a zonal direction. At 500 m depth, density is almost uniform in the Northern Hemisphere and a gradual density gradient is observed south of 10°S latitude. There is no appreciable change in F_t values in the model domain at 1000 m depth.

Computed currents and sea surface topography during winter

The diagnostic calculations of currents and sea surface topography are depicted in Fig. 3 and Fig.4 respectively. The surface circulation at 20 m depth (Fig. 3a) shows the presence of major persistent currents during winter. The westward flowing South and North Equatorial Currents (SEC and NEC) are observed across the entire model domain between 10°S and 20°S and 0° and 10°N respectively. Off the coasts of Somalia, most of the water from NEC turns south, crosses the equator and forms the

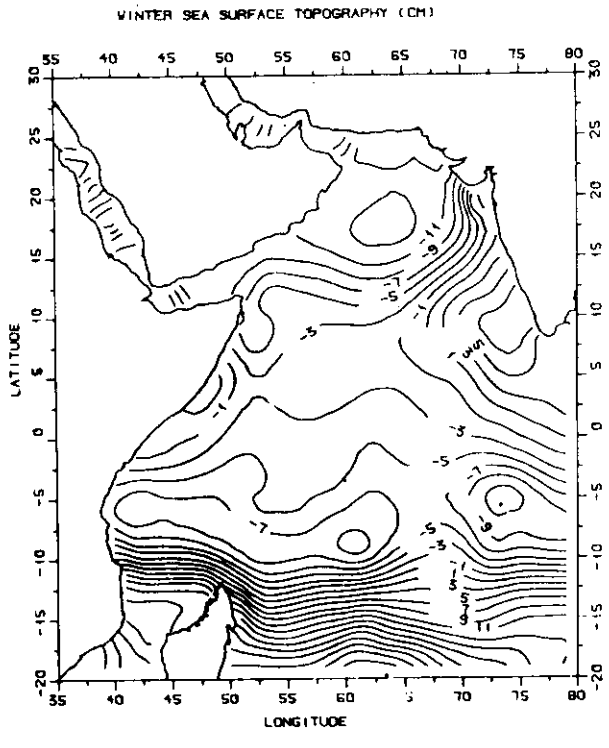

Fig. 4—Computed sea surface topography (cm) during winter season.

Equatorial Counter Current (ECC). In fact, the eastward flowing ECC, fed jointly by the southward flowing Somali Current (SC) and SEC, is observed between 10°S and 3°S. The southward flowing SC attains a maximum velocity of 75 cm sec^{-1}. The Arabian Sea north of the equator is mainly covered by weak westward and southwestward flowing NE monsoon current. All the major currents at 20 m depth are in consistent with the ship drift currents compiled by Cutler & Swallow[12]. The sea surface topography contours in Fig.4 shows SEC, southward flowing Somali Current and eastward flowing ECC fed by East African Coastal Current (EACC) and Somali Current. Along the west coast of India, the sea level is high and hence a northward flow is found in this region.

At 50 m depth, there is an appreciable change in flow north of 10°N in the Arabian Sea compared to the flow at 20 m depth. In the Southern Hemisphere, all the major currents such as the SEC, ECC and the southward flowing SC are still persisting; however, the intensity of all these currents are further reduced. The NEC and ECC ranges between 0° and 5°N and 2°S and 7°S respectively. The SEC and southward flowing SC are observed at 150 and 300 m depths also. At these depths, the ECC is replaced by an Equatorial Under Current (EUC), which is mainly located in the equatorial region at the western part of the model domain. The northern Arabian Sea between 12°N and 22°N is covered by a cyclonic circulation at 150 and 300 m depths. The circulation pattern has completely changed at 500 and 1000 m depths (Fig. 3e-f) compared to the upper levels. At 500 m depth, SEC is shifted more towards south and its intensity is further reduced. At 1000 m depth, SEC is almost vanished. The entire model domain is covered by eddy-like circulation features at these depths.

Results of semi-diagnostic calculations of currents in the western tropical Indian Ocean

In the semi-diagnostic model, two more equations namely the turbulent diffusion equations of heat and salt are included along with the diagnostic model equations.

The equations of heat and salt used are:

$$\frac{\partial T}{\partial t} + AT = \frac{\partial \left[\nu_T \frac{\partial T}{\partial z} \right]}{\partial z} + \mu_T \Delta T \qquad \ldots (11)$$

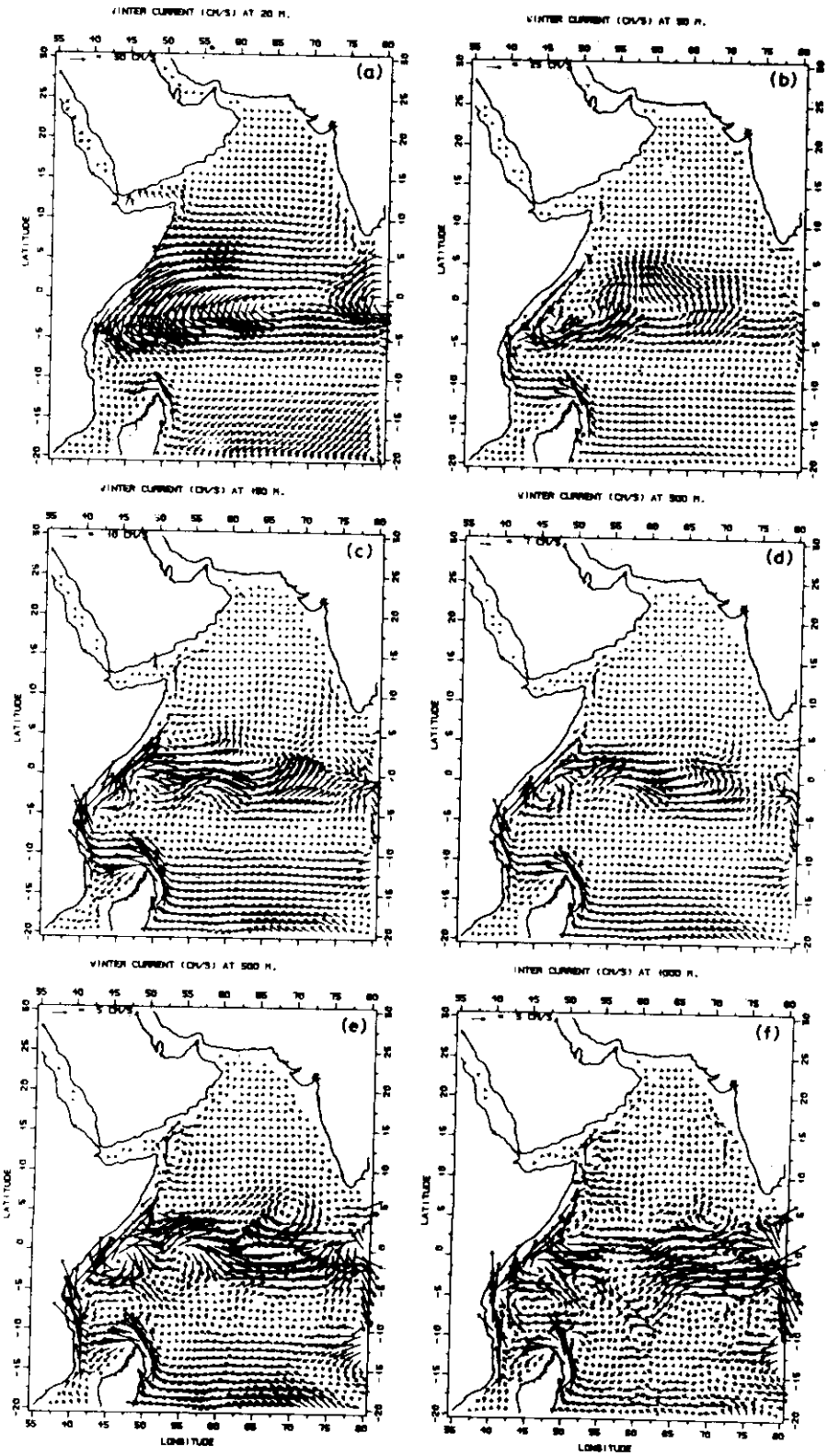

Fig. 5—Hydrodynamically adjusted currents (cm sec^{-1}) during winter season using semi-diagnostic model at (a) 20 m depth (b) 50 depth (c) 150 m (d) 300 m (e) 500 m (f) 1000 m depths.

$$\frac{\partial S}{\partial t} + AS = \frac{\partial\left[\nu_T \frac{\partial S}{\partial z}\right]}{\partial z} + \mu_T \Delta S \qquad \ldots (12)$$

where μ_T, ν_T are horizontal and vertical turbulent diffusion coefficients of heat and salt.

The steady state solution of the semi-diagnostic model equations is obtained in two stages: during the first diagnostic stage, all the equations except the turbulent diffusion equations of heat and salt were solved with appropriate boundary and initial conditions. Equation of state is used only to compute the density field and the same is kept constant throughout the first stage of model integration. The model is integrated for approximately one month by which time the flow fields are generated completely. During the second stage which is called adaptation stage, all the model equations including the turbulent diffusion equations of heat and salt were again integrated for approximately one more month, with the initial conditions for flow fields obtained from the first diagnostic stage. The initial conditions for temperature and salinity during the adaptation stage are the original temperature and salinity data that were used for the diagnostic calculations. During the adaptation stage, the input of density field was allowed to vary for a while, and the flow fields and other hydrological variables were hydrodynamically adjusted with wind field and bottom topography. The parameter values used for the horizontal eddy diffusivity and vertical eddy diffusivity coefficients are 5×10^8 cm^2 sec^{-1} and 10 cm^2 sec^{-1} respectively.

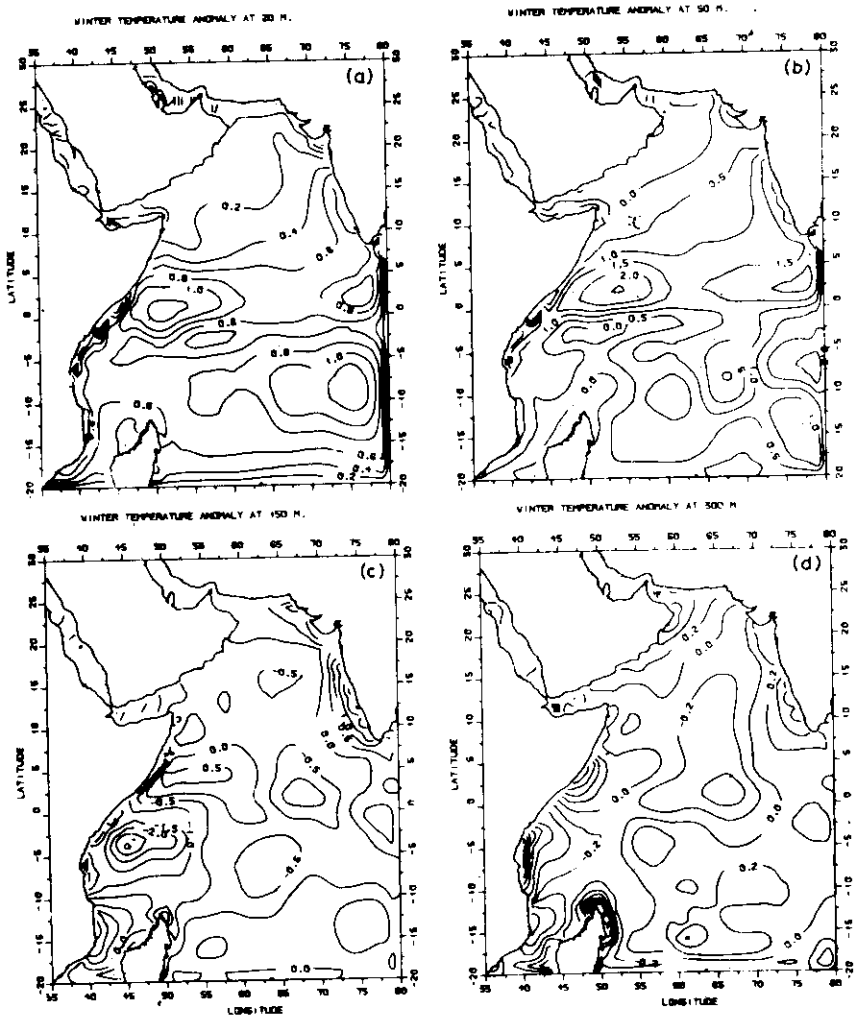

Fig. 6—Temperature anomaly fields at (a) 20 m (b) 50 m (c) 150 m (d) 300 m depths.

The wind stress and temperature and salinity data used to drive the model are obtained from Hellerman & Rosenstein[10] and Levitus[11] respectively.

Hydrodynamic adjustment of the temperature, salinity and flow fields

One of the disadvantages of purely diagnostic models is that the input of density field (temperature and salinity) contains of "noise" effects of stationary processes. This would lead to distortions in the climatic currents which are to be calculated. In addition, the specified density fields do not adjust with bottom topography and wind field. So, it is necessary to hydrodynamically adjust the input of density with bottom topography and wind field. In semi-diagnostic model, we imposed the specified temperature and salinity fields and flow fields calculated by the first diagnostic stage as initial approximations for the adjustment process. The flow fields, temperature and salinity fields were found to be hydrodynamically adjusted after 30 days of model integration from the diagnostic stage.

Hydrodynamically adjusted flow fields

Figure 5 shows the hydrodynamically adjusted flow fields at 20, 50, 150, 300, 500 and 1000 m depths. A comparison of Fig.5a with Fig.3a shows that the circulation is more smoothed in the entire model domain during the adjustment process. The intensity of currents along the Somalia coast and in the equatorial regions has been reduced considerably after the adaptation stage. The southward flowing Somali Current now attains a

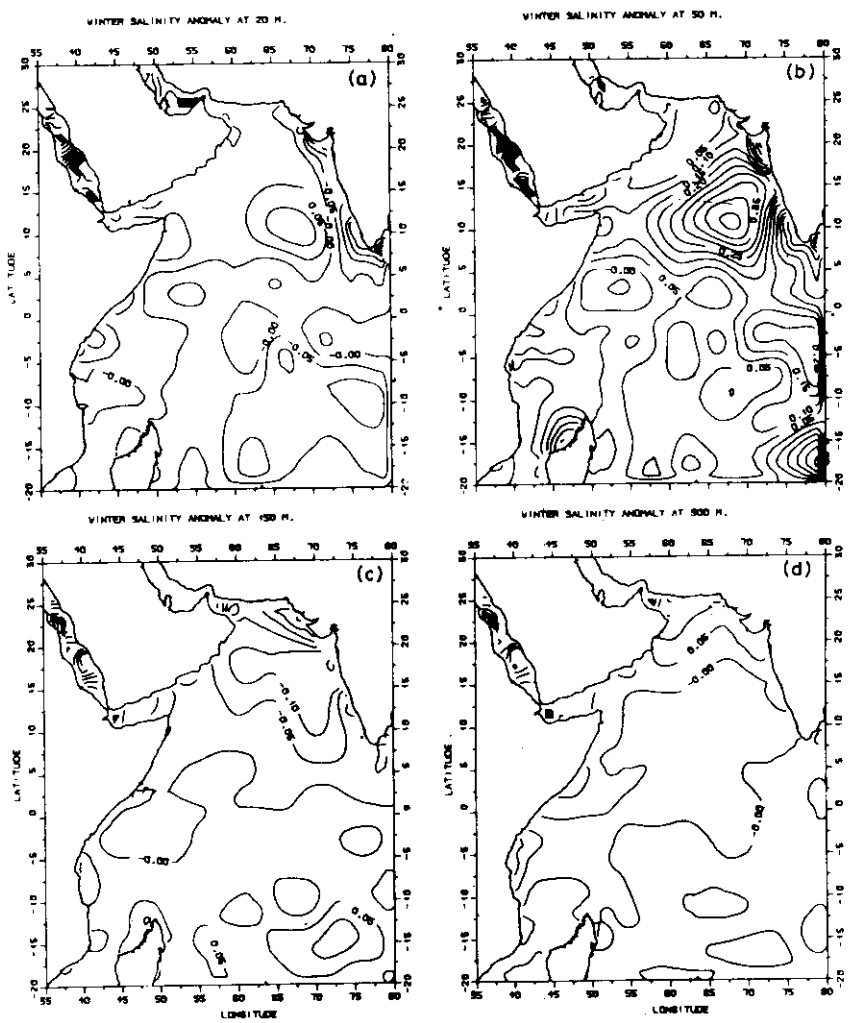

Fig. 7 —Salinity anomaly fields at (a) 20 m (b) 50 m (c) 150 m (d) 300 m depths.

maximum velocity of 60 cm sec^{-1}. Qualitatively, the circulation features have not changed much at 20 m depth during the adjustment stage.

At 50 m depth, the southward flowing Somali Current and ECC are well pronounced in Fig. 5b compared to Fig.3b. The south eastern sector of Arabian Sea shows an anticyclonic eddy in Fig. 5b and the same is not clear in Fig. 3b. It is found that at 150 and 300 m, the velocity fields were smoothed and unrealistic currents were removed in the Somali and equatorial regions after the adaptation process. The anticyclonic eddy observed in the eastern Arabian Sea at 50 m depth can be seen at 150 m depth also. However, at 300 m depth, the same eddy is shifted more towards south and takes position in the eastern part of central Indian Ocean. At 500 and 1000 m depth also, the currents have been considerably smoothed (Fig. 5e-f) in the entire model domain during the adjustment process. At these depths, the flow all along the Somali coast has changed its direction to northwards and the southward flow is confined only to the northern tip of Somali coast. The anticyclonic eddy observed at the eastern part of equatorial Indian Ocean at 300 m depth is found at 500 and 1000 m depth also.

Adjustment of temperature and salinity fields

The hydrodynamic adjustment of temperature and salinity fields at selected depths are presented in the form of anomaly diagrams. The anomaly of a particular variable is equal to the difference between the observed variable and adjusted variable. The temperature and salinity anomaly fields at 20, 50, 150 and 300 m depths are represented in (Fig. 6a-d) and (Fig. 7a-d) respectively. Temperature anomaly fields at 20 and 50 m depths (Fig. 6a,b) show only positive values. At 20 m depth, the positive anomaly reaches a maximum value of about 1.0°C, whereas, at 50 m depth, it attains a maximum value of about 20°C. At 300 m depth, temperature anomaly field shows both positive and negative values. The temperature anomaly fields represented by (Fig. 6a-d) show that the climatic temperature data used to drive the model was smoothed hydrodynamically during the adjustment process. The salinity anomaly fields show that the data was smoothed much at 50 m depth compared to all the other depths. Salinity anomaly field at 20 m depth shows both positive and negative values, whereas 50 m depth is covered by mainly positive values. Salinity anomaly fields at 150 and 300 m depths (Fig. 7d) show that the climatic salinity values have not changed much after the adjustment process.

Acknowledgement

One of the authors (C.Shaji) is indebted to the Council of Scientific & Industrial Research, New Delhi for financial assistance.

References

1 Sarkisyan A S, *Theory and calculations of ocean currents*, (U S Department of Commerce and the National Science Foundation, Washington D C) 1969.
2 Bulatov R P, Demin Yu L & Pogarkov S G, *Oceanologia*, 6 (1975) 995.
3 Demin Yu L, *Meteorologia i Hydrologia*, 1 (1975) 48.
4 Demin Yu L, *Fir Atmos i Okeana*, 11, 5 (1975) 534.
5 Sarkisyan A S, *The sea:marine modelling*, Vol 6 (J Willey, New York) 1977, 363.
6 Sarkisyan A S & Demin Yu L, *Large scale oceanographic experiments*, (WCRP Publication Series, Tokyo) 2(1) (1983), 201.
7 Marchuk G I & Sarkisyan A S, *Mathematical modelling of ocean circulation*, (Springer-Verlag, Berlin) 1988, 292.
8 Gill A E, *Atmosphere-ocean dynamics*, (Academic Press, New York), 1982, pp 662.
9 Bahulayan N & Shaji C, *Proc Indian Nat Sci Acad (Physical Sciences)*, 62, A(4) (1996) 325.
10 Hellerman S & Rosenstein M, *J Phys Oceanogr*, 13, 7 (1983) 1093.
11 Levitus S, *Climatological atlas of the world ocean*, NOAA prof. paper 13 (US Government Printing Office, Washington D C) 1982, pp 173.
12 Cutler A N & Swallow J C, *Surface currents of the Indian Ocean* (Institute of Oceanographic Sciences,U K) 1984, pp 8.